New Journal of Physics
The open-access journal for physics

Fast transport of Bose–Einstein condensates

E Torrontegui[1], Xi Chen[1,2], M Modugno[3,4], S Schmidt[5], A Ruschhaupt[5] and J G Muga[1,6,7]

[1] Departamento de Química Física, Universidad del País Vasco—Euskal Herriko Unibertsitatea, Apdo. 644, Bilbao, Spain
[2] Department of Physics, Shangai University, 200444 Shanghai, People's Republic of China
[3] Departamento de Física Teórica e Historia de la Ciencia, Universidad del País Vasco—Euskal Herriko Unibertsitatea, Apdo. 644, Bilbao, Spain
[4] IKERBASQUE, Basque Foundation for Science, 48011 Bilbao, Spain
[5] Institut für Theoretische Physik, Leibniz Universität Hannover, Appelstraße 2, 30167 Hannover, Germany
[6] Max Planck Institute for the Physics of Complex Systems, Nöthnitzer Str. 38, 01187 Dresden, Germany
E-mail: jg.muga@ehu.es

New Journal of Physics **14** (2012) 013031 (11pp)
Received 5 October 2011
Published 18 January 2012
Online at http://www.njp.org/
doi:10.1088/1367-2630/14/1/013031

Abstract. We propose an inverse method to accelerate without final excitation the adiabatic transport of a Bose–Einstein condensate. The method is based on a partial extension of the Lewis–Riesenfeld invariants and provides transport protocols that satisfy exactly the no-excitation conditions without approximations. This inverse method is complemented by optimizing the trap trajectory with respect to different physical criteria and by studying the effect of perturbations such as anharmonicities and noise.

[7] Author to whom any correspondence should be addressed.

Contents

1. Introduction

A major goal of atomic physics is the comprehensive control of the atomic quantum state for fundamental research and applications in interferometry, metrology or information processing. The ability to manipulate Bose–Einstein condensates (BECs) may be particularly rewarding due, for example, to their potential use in interferometric sensors, but it is also challenging, as their low temperatures make them more fragile than ordinary cold atoms. A basic operation is the transport of the condensate to appropriate locations such as a 'science chamber', or to launch or stop the atomic cloud. This transport has been performed with several techniques based on adiabatic, slow motion to avoid excitations and losses [1–4]. Long transport times, however, may be counterproductive since the condensate is more exposed to noise and decoherence, and also limit severely the repetition rates and signal-to-noise ratios. Fast, non-adiabatic but 'faithful' transport of cold atoms, i.e. leading to the desired final state, has also been investigated experimentally [5] and theoretically [6–8]. For the Schrödinger equation (SE) an inverse engineering method based on constructing Lewis–Riesenfeld invariants and corresponding dynamical modes (solutions of the SE formed by invariant eigenvectors times a phase factor) provides a 'shortcut to adiabaticity' [9, 10]. However, the invariant concept is not directly applicable to the nonlinear Gross–Pitaevskii equation (GPE). In fact, previous extensions of this inverse technique to expansions of condensates required special regimes or time-dependent Feshbach resonance control [11–13].

In this paper, we propose a method for accelerating without final excitation the adiabatic transport of a BEC, by generalizing the invariant-based inverse engineering approach [9]; see section 3. This method will be illustrated with a numerical example and compared with a direct (as opposed to 'inverse') approach. In section 4, we shall optimize the trap trajectory according to several criteria, since the invariant-based inverse engineering provides a family of possible transport solutions. The effect of anharmonicities in the potential and the effect of noise on the transport process will be studied in section 5.

2. General theory

Our starting point is the GPE for potentials whose Schrödinger (linear) dynamics admit a quadratic invariant in momentum [8, 14–17],

$$\mathrm{i}\hbar\frac{\partial\psi(\mathbf{q},t)}{\partial t}=\left[-\frac{\hbar^2}{2m}\nabla_{\mathbf{q}}^2-\mathbf{F}(t)\cdot\mathbf{q}+\frac{1}{2}m\omega^2(t)|\mathbf{q}|^2\right.$$
$$\left.+\frac{1}{\rho^2}U\left(\frac{\mathbf{q}-\boldsymbol{q}_{\mathrm{c}}}{\rho}\right)+g_D|\psi(\mathbf{q},t)|^2+f(t)\right]\psi(\mathbf{q},t), \tag{1}$$

where $f=f(t)$ is arbitrary, $\nabla_{\mathbf{q}}^2$ is the Laplacian in Cartesian coordinates for $D=1$, 2 or 3 dimensions, U is an arbitrary potential function of the argument $\boldsymbol{\sigma}\equiv(\mathbf{q}-\boldsymbol{q}_{\mathrm{c}})/\rho$ and $\omega(t)$, the force $\mathbf{F}(t)$, $\boldsymbol{q}_{\mathrm{c}}(t)$ and the scaling function $\rho(t)$ satisfy

$$\omega_0^2/\rho^3(t)=\ddot{\rho}(t)+\omega^2(t)\rho(t), \tag{2}$$

$$\mathbf{F}(t)/m=\ddot{\boldsymbol{q}}_{\mathrm{c}}(t)+\omega^2(t)\boldsymbol{q}_{\mathrm{c}}(t), \tag{3}$$

where ω_0 is a constant and the dots represent time derivatives. The physical meaning of $\boldsymbol{q}_{\mathrm{c}}$ depends on the process type; see [8] and further details below. For rigid harmonic transport it becomes a classical trajectory of the center of mass and for anharmonic transport with a compensating force it is the transport function of the trap. The wave function is normalized to one. Without the nonlinear term ($g_D=0$), it follows from the Lewis–Riesenfeld invariant theory [18, 19] that the solution can be written as

$$\psi(\mathbf{q},t)=\rho^{-D/2}\,\mathrm{e}^{\frac{\mathrm{i}m}{\hbar\rho}[\dot{\rho}|\mathbf{q}|^2/2+(\dot{\boldsymbol{q}}_{\mathrm{c}}\rho-\boldsymbol{q}_{\mathrm{c}}\dot{\rho})\cdot\mathbf{q}]}$$
$$\times\exp\left\{-\frac{\mathrm{i}}{\hbar}\int_0^t\mathrm{d}t'\left[\frac{m\left(|\dot{\boldsymbol{q}}_{\mathrm{c}}\rho-\boldsymbol{q}_{\mathrm{c}}\dot{\rho}|^2-\omega_0^2|\boldsymbol{q}_{\mathrm{c}}|^2/\rho^2\right)}{2\rho^2}+f(t')\right]\right\}\phi(\boldsymbol{\sigma},\tau), \tag{4}$$

where we have introduced a scaled time $\tau(t)=\int_0^t\mathrm{d}t'\rho^{-2}(t')$, and $\phi(\boldsymbol{\sigma},\tau)$ satisfies an SE with a time-independent Hamiltonian.

These results can be generalized partially for the GPE, and the extent of the generalization depends on the process type. Inserting (4) as an ansatz for a time-dependent solution of the GPE, $\phi(\boldsymbol{\sigma},\tau)$ must satisfy

$$\mathrm{i}\hbar\frac{\partial\phi}{\partial\tau}(\boldsymbol{\sigma},\tau)=\left[-\frac{\hbar^2}{2m}\nabla_{\boldsymbol{\sigma}}^2+\frac{m\omega_0^2}{2}|\boldsymbol{\sigma}|^2+U(\boldsymbol{\sigma})+\rho^{2-D}g_D|\phi(\boldsymbol{\sigma},\tau)|^2\right]\phi(\boldsymbol{\sigma},\tau). \tag{5}$$

Equation (5) is very general and applicable to compressions, expansions or transport driven by harmonic or anharmonic potentials. It is most useful when $\rho^{2-D}g_D$ does not depend on time, since the physical solution of the time-dependent problem is then mapped, via (4), to the solution of a much simpler stationary equation. This happens in several physically relevant cases, in particular for expansions of BECs when $D=2$, or by tuning g_D as a time-dependent coupling to cancel the time dependence of ρ^{2-D} [11]. Different time scalings combined with a Thomas–Fermi approximation also lead to a stationary equation [11].

3. Transport processes

Here we are interested in the simple but very important case $\rho(t) = 1$, $\forall t$, associated with transport processes driven by a rigidly displaced harmonic potential. Then $\tau = t$, $\omega(t) = \omega_0$ and the coefficients of (5) are time independent. It is also useful to define $\phi(\boldsymbol{\sigma}, t) = \mathrm{e}^{-\mathrm{i}\mu t/\hbar}\chi(\boldsymbol{\sigma})$, where μ is the chemical potential and $\chi(\boldsymbol{\sigma})$ satisfies the stationary GPE

$$\left[-\frac{\hbar^2}{2m}\nabla_\sigma^2 + \frac{m\omega_0^2}{2}|\boldsymbol{\sigma}|^2 + U(\boldsymbol{\sigma}) + g_D|\chi(\boldsymbol{\sigma})|^2\right]\chi(\boldsymbol{\sigma}) = \mu\,\chi(\boldsymbol{\sigma}). \tag{6}$$

The solution of the time-dependent GPE equation for a single transport mode with the initial condition $\psi(\mathbf{q}, 0) = \exp[(\mathrm{i}/\hbar)m\dot{\boldsymbol{q}}_\mathrm{c}(0)\cdot\mathbf{q}]\chi(\boldsymbol{\sigma})$, where $\chi(\boldsymbol{\sigma})$ is given by (6), is

$$\psi(\mathbf{q}, t) = \exp\left\{\frac{\mathrm{i}}{\hbar}(-\mu t + m\dot{\boldsymbol{q}}_\mathrm{c}\cdot\mathbf{q}) - \frac{\mathrm{i}}{\hbar}\int_0^t \mathrm{d}t'\left[\frac{m}{2}(|\dot{\boldsymbol{q}}_\mathrm{c}|^2 - \omega_0^2|\boldsymbol{q}_\mathrm{c}|^2) + f(t')\right]\right\}\chi(\boldsymbol{\sigma}) \tag{7}$$

with $\boldsymbol{\sigma} = \mathbf{q} - \mathbf{q}_\mathrm{c}$. Equation (7) is an exact solution of the GPE as can be checked by direct substitution. It is a fundamental result since this wave function is shape invariant and the only possible excitations associated with such a mode are center of mass oscillations with constant mean field energy. As we are interested in the transport between an initial point and a final point, we restrict the analysis in the following to the one-dimensional (1D) transport scenario between these two points and omit the vector notation.

3.1. Inverse engineering of harmonic transport

For a 1D, harmonic and horizontal transport of a condensate from 0 to d in a time t_f, with zero mean velocity at $t = 0$ and t_f, q_c (now a scalar function) must be chosen to match the transport mode (7) with the instantaneous eigenstates of the Hamiltonian, including the mean field term, at times $t = 0$ and $t = t_f$.

A concrete example will illustrate how this works. Consider an ^{87}Rb BEC in the $F = 2$, $m_f = 2$ ground state constituted by 3000 atoms [2]. The transport of BECs aided by microchips can use a 'bucket chain' [20] or a single harmonic and frequency-stable bucket [21]. We assume here a single bucket with $\omega_0 = 2\pi \times 50\,\mathrm{Hz}$ moved from $q_0(0) = 0$ at time $t = 0$ to $q_0(t_f) = d = 1.6\,\mathrm{mm}$ at t_f along the transport function $q_0(t)$. The time-dependent GPE for $\psi(q, t)$ is now

$$\mathrm{i}\hbar\frac{\partial\psi}{\partial t}(q, t) = \left[-\frac{\hbar^2}{2m}\nabla_q^2 + \frac{m\omega_0^2}{2}(q - q_0)^2 + g_1|\psi(q, t)|^2\right]\psi(q, t), \tag{8}$$

a particular case of (1) with $\omega(t) = \omega_0$, $U = 0$, $F(t) = m\omega_0^2 q_0(t)$, $f(t) = m\omega_0^2 q_0^2(t)/2$ and $\rho(t) = 1$, so (2) does not play any role. The 1D version of (7) in this case is

$$\psi(q, t) = \exp\left\{\frac{\mathrm{i}}{\hbar}(-\mu t + m\dot{q}_\mathrm{c}q) - \frac{\mathrm{i}}{\hbar}\int_0^t \mathrm{d}t'\left[\frac{m}{2}\left(\dot{q}_\mathrm{c}^2 - \omega_0^2(q_\mathrm{c}^2 - q_0^2)\right)\right]\right\}\chi(\sigma), \tag{9}$$

and $q_\mathrm{c}(t)$ has to satisfy

$$\ddot{q}_\mathrm{c}(t) + \omega_0^2[q_\mathrm{c}(t) - q_0(t)] = 0, \tag{10}$$

the equation for a classical trajectory $q_\mathrm{c}(t)$ in a moving harmonic potential. (Note that for an abrupt shift of the trap, one recovers the scaling for dipole oscillations [22].)

If we impose at $t = 0$ the initial conditions

$$q_c(0) = \dot{q}_c(0) = \ddot{q}_c(0) = 0, \tag{11}$$

the transport modes (7) become equal to the instantaneous eigenstates of (8) at $t = 0$.

To solve (8) we proceed in two different ways, namely using direct and inverse approaches.

In the direct approach we fix first the evolution of the center of the trap $q_0(t)$. In [2], for example, see figure 5 there, $\dot{q}_0(t)$ is increased linearly during a quarter of the transported distance $d/4$, then kept constant for $d/2$ and finally ramped back to zero during the last quarter,

$$q_0(t) = \begin{cases} \dfrac{v_m^2 t^2}{d}, & 0 < t < \dfrac{d}{2v_m}, \\ v_m t - \dfrac{d}{4}, & \dfrac{d}{2v_m} < t < \dfrac{d}{v_m}, \\ \dfrac{v_m}{2(d/v_m - t_f)}(t - t_f)^2 + d, & \dfrac{d}{v_m} < t < t_f, \end{cases}$$

where $v_m = 3d/(2t_f)$ is the maximum trap velocity during the transport compatible with $q_0(t_f) = d$ in this scheme. Solving (10) for the previous $q_0(t)$ with initial conditions $q_c(0) = \dot{q}_c(0) = 0$ and imposing continuity on $q_c(t)$ and $\dot{q}_c(t)$, we find that

$$\begin{aligned} q_c(t_f) - q_0(t_f) &= 9d(1 - 2\cos\varphi)(\sin^2\varphi)/(\omega_0^2 t_f^2), \\ \dot{q}_c(t_f) - \dot{q}_0(t_f) &= \frac{9d}{2\omega_0 t_f^2}(\sin\varphi + \sin 2\varphi - \sin 3\varphi), \end{aligned} \tag{12}$$

where $\varphi = \omega_0 t_f/3$. The final state of the transported BEC is given by (7) and (12). In general, some excitation is produced, except for the discrete set of final times $t_{f,N} = 3(2N+1)\pi/\omega_0$, $N = 0, 1, 2, \ldots$, for which

$$q_c(t_f) = d, \quad \dot{q}_c(t_f) = \ddot{q}_c(t_f) = 0, \tag{13}$$

and the transported state matches the eigenstate of the final Hamiltonian. The classically moving center of mass and the trap center stop at d, $\dot{q}_c(t_f) = 0$, $\dot{q}_0(t_f) = 0$, with zero (classical) energy $m\dot{q}_c(t_f)^2/2 + m\omega_0^2[d - q_c(t_f)]^2/2 = 0$. Using this direct approach, the minimal final time which does not produce excitation is $t_{f,0} = 3\pi/\omega_0$ ($N = 0$). In our example, $t_{f,0} = 30\,\text{ms}$. For such short times the transport is not adiabatic.

Thanks to the structure of the solution (7), we may apply a generalized inverse engineering method similar to the one for the linear case [8, 9, 11]. The idea is to design $q_c(t)$ first and deduce the transport protocol from it. We impose the conditions (11) and (13) at $t = 0$ and t_f, and interpolate q_c with a function, e.g. a polynomial with enough parameters to satisfy all these conditions. Then $q_0(t)$ is calculated via (10). An example is shown in figure 1 where we have chosen $t_f = 20\,\text{ms} < t_{f,0}$. By construction no final excitation is produced, and the final fidelity (overlap between the transported state and the ground state at t_f) is one. Contrast this to the direct approach which, for $t_f = 20\,\text{ms}$, produces more transient excitation and a final excited state with nearly zero fidelity.

In principle, there is no lower limit to t_f with the inverse method, but in practice there are some limitations [8]. Smaller values of t_f increase the distance from the condensate to the trap center, see (12), and the effect of anharmonicity. There could also be geometrical constraints: for short t_f, $q_0(t)$ could exceed the interval $[0, d]$. For the polynomial ansatz this happens [8]

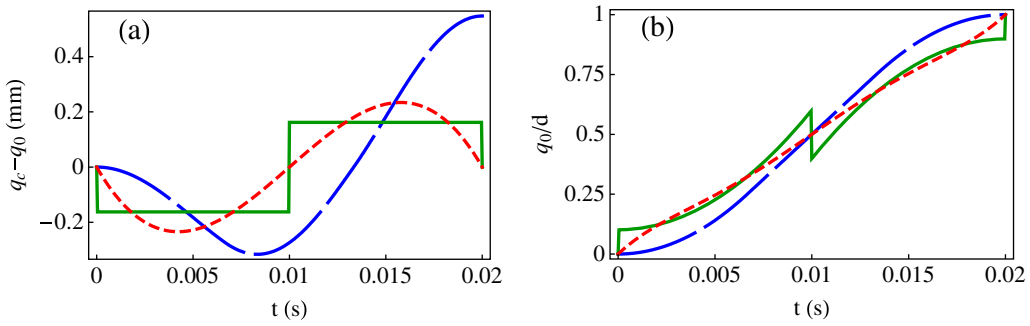

Figure 1. (a) Displacement $q_c - q_0$ versus time. Blue long-dashed line: direct method; red short-dashed line: inverse method (polynomial). Solid green line: inverse method + OCT. (b) Trap trajectories. Parameter values: $d = 1.6\,\text{mm}$, $t_f = 20\,\text{ms}$, $\delta \simeq 0.162\,\text{mm}$ and $\omega_0 = 2\pi \times 50\,\text{Hz}$.

at $t_f = 2.505/\omega_0$, $t_f \approx 8\,\text{ms}$ for the parameters of the example. Optimal control theory (OCT) combined with the inverse method, see below, provides a way of designing trajectories taking these restrictions into account.

3.2. Anharmonic transport

The inverse method can also be applied to anharmonic transport by means of a compensating force [8] which could be implemented by means of a magnetic field gradient [23]. Let the anharmonic potential be $U(q)$ at time $t = 0$ and $U(q - d)$ at time t_f. The condensate starts in the ground state of the potential at time $t = 0$. We set $q_0(t) = q_c(t)$, $\omega(t) = \omega_0 = 0$, $f = 0$ and $F(t) = m\ddot{q}_0(t)$ in (1), so the GPE for $\psi(q, t)$ becomes

$$\mathrm{i}\hbar\frac{\partial\psi}{\partial t}(q,t) = \left[-\frac{\hbar^2}{2m}\nabla_q^2 - m\ddot{q}_0 q + U(q - q_c) + g_1|\psi(q,t)|^2\right]\psi(q,t),$$

and the auxiliary equations (2) and (3) are satisfied trivially. Here we impose

$$q_0(0) = 0, \quad \dot{q}_0(0) = 0, \quad q_0(t_f) = d, \quad \dot{q}_0(t_f) = 0.$$

We may optionally impose also $\ddot{q}_0(t) = 0$ at $t = 0$ and t_f. The function that must be interpolated is now $q_0(t)$, and again we may consider a polynomial. Note that the exact potential U could be unknown because $q_0(t)$ is independent of U. By implementing the compensating force $m\ddot{q}_0(t)$, we ensure that the condensate will be in the ground state of the moved trap at final time t_f.

As an example, let $t_f = 20\,\text{ms}$ and $d = 1.6\,\text{mm}$; then we get for the compensating acceleration $\ddot{q}_0(t) \leqslant 23.1\,\text{m}\,\text{s}^{-2}$ for $0 \leqslant t \leqslant t_f$.

4. Optimal control theory

Given the freedom left by the inverse method, it is natural to combine it with OCT and design the trajectory according to relevant physical criteria [24]. For harmonic transport, we have imposed the boundary conditions (11) and (13) at $t = 0$ and t_f, but $q_0(t)$ and the polynomial ansatz for $q_c(t)$ are quite arbitrary. As an example of the possibilities of OCT, suppose that we wish to limit the deviation of the condensate from the trap center according to $-\delta \leqslant q_c - q_0 \leqslant \delta$, $\delta > 0$

and find the minimal time t_f. The transport process given by (7), (11) and (13) can be rewritten as a minimum-time optimal control problem defining the state variables $x_1(t)$ and $x_2(t)$ and the control $u(t)$,

$$x_1 = \alpha, \quad x_2 = \dot{\alpha}, \quad u(t) = \alpha - q_0. \tag{14}$$

Equation (10) is transformed into a system of equations,

$$\dot{x}_1 = x_2, \quad \dot{x}_2 + \omega_0^2 u = 0. \tag{15}$$

The OCT problem is to find $-\delta \leqslant u(t) \leqslant \delta$ with $u(0) = u(t_f) = 0$, $\{x_1(0), x_2(0)\} = \{0, 0\}$ and $\{x_1(t_f), x_2(t_f)\} = \{d, 0\}$ in the minimum final time t_f. The optimal control Hamiltonian [25] is $H_c = p_1 x_2 - p_2 \omega_0^2 u$, where p_1 and p_2 are conjugate variables. The Pontryagin maximality principle [25] tells us that for $u(t)$, $\mathbf{x}(t)$ to be time optimal, it is necessary that there exists a non-zero, continuous vector $\mathbf{p}(t)$ such that $\dot{\mathbf{x}} = \partial H_c/\partial \mathbf{p}$, $\dot{\mathbf{p}} = -\partial H_c/\partial \mathbf{x}$ at any instant, the value of the control maximizes H_c, and $H_c(\mathbf{p}(t), \mathbf{x}(t), \mathbf{u}(t)) = c \geqslant 0$, with c being a constant.

The solution is of bang–bang type [26],

$$u(t) = \begin{cases} 0, & t \leqslant 0, \\ -\delta, & 0 < t < t_1, \\ \delta, & t_1 < t < t_f, \\ 0, & t \geqslant t_f, \end{cases}$$

where the initial and final discontinuities are chosen to satisfy the boundary conditions. Solving the system (15) and imposing continuity on x_1 and x_2, one finds for the switching and final times

$$t_1 = t_f/2, t_f = 2(d/\delta)^{1/2}/\omega_0.$$

The trap trajectory is deduced from (14),

$$q_0(t) = \begin{cases} 0, & t \leqslant 0, \\ (1 + \omega_0^2 t^2/2)\delta, & 0 < t < t_1, \\ -[\omega_0^2 (t - t_f)^2/2 + 1]\delta + d, & t_1 < t < t_f, \\ d, & t \geqslant t_f. \end{cases}$$

In figure 1, the displacement of the center of mass with respect to the trap center and the trap trajectory is plotted for this optimal trajectory. We have chosen $\delta \simeq 0.162\,\text{mm}$ so that the minimal final time is $t_f = 20\,\text{ms}$ as in the previous example.

Another important constraint might be that the center of the physical trap stays inside a given range (e.g. inside the vacuum chamber), i.e. the constraint is then $q_\downarrow \leqslant q_0(t) \leqslant q_\uparrow$. Following the OCT procedure, we finally get

$$q_0(t) = \begin{cases} 0, & t \leqslant 0, \\ q_\uparrow, & 0 < t < t_1, \\ q_\downarrow, & t_1 < t < t_f, \\ d, & t \geqslant t_f. \end{cases}$$

where

$$\omega_0 t_1 = \arccos\left[1 - \frac{q_\downarrow d - d^2/2}{q_\uparrow (q_\downarrow - q_\uparrow)}\right],$$

$$\omega_0 t_f = \omega_0 t_1 + \arccos\left[\frac{q_\downarrow d - d^2/2 - q_\downarrow (q_\downarrow - q_\uparrow)}{(d - q_\downarrow)(q_\downarrow - q_\uparrow)}\right].$$

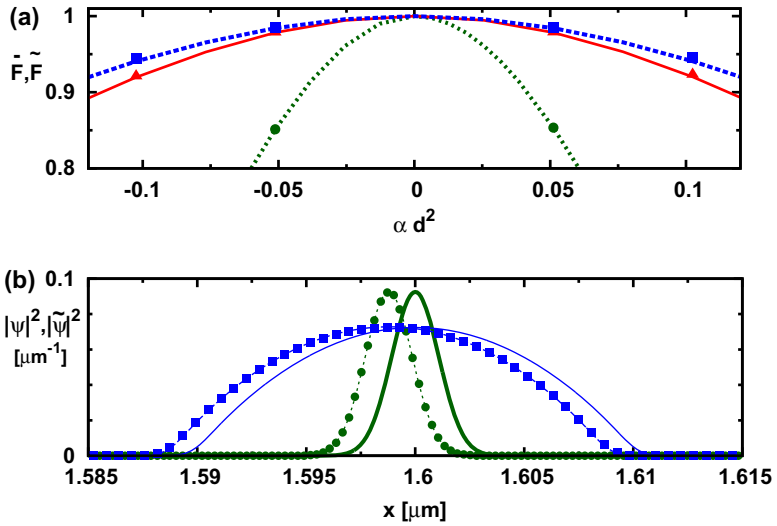

Figure 2. Effect of trap anharmonicity α on transport. (a) Exact fidelity $\bar{F}$ (lines)—solving the GPE equation—and approximated fidelity $\tilde{F}$ (symbols); $g_1 = 0$ (green dotted lines and circles), $g_1/\hbar = 0.05\,\mathrm{m\,s^{-1}}$ (red solid lines and triangles) and $g_1/\hbar = 0.1\,\mathrm{m\,s^{-1}}$ (blue dashed lines and boxes). (b) Wave function at final time t_f; $g_1 = 0$, $\alpha = 0$ (green thick solid line, scaled by a factor of 4), $g_1 = 0$, $\alpha d^2 = 0.0512$ (exact result ψ: green thin dashed line, approximation $\tilde{\psi}$: green circles, scaled by a factor of 4), $g_1/\hbar = 0.1\,\mathrm{m\,s^{-1}}$, $\alpha = 0$ (blue thin solid line), $g_1/\hbar = 0.1\,\mathrm{m\,s^{-1}}$, $\alpha d^2 = 0.0512$ (exact result ψ: blue dashed line, indistinguishable in the scale of the figure from the approximation $\tilde{\psi}$: blue boxes); $d = 1.6\,\mathrm{mm}$, $t_f = 20\,\mathrm{ms}$ and $\omega_0 = 2\pi \times 50\,\mathrm{Hz}$.

At the beginning the trap is immediately set at the upper bound $q_\uparrow$ to accelerate the condensate as much as possible and at time t_1 the trap is moved to the lower bound $q_\downarrow$ to decelerate the condensate so as to leave the condensate at rest at the final time t_f.

5. Effect of perturbations

First we investigate the effect of anharmonicities when the harmonic transport protocol is applied. For a symmetrically perturbed potential

$$V = \omega_0^2 m[(q - q_0)^2 + \alpha(q - q_0)^4]/2, \tag{16}$$

the results can be seen in figure 2(a) where we compare approximate results, see below, with exact numerical solutions of the GPE where the wavefunction coincides with the initial wavefunction of the harmonic trap at $t = 0$ (this is a very good approximation since the anharmonicity only becomes relevant during the transport process). For small anharmonicity α we still get a very high fidelity $\bar{F} = |\langle\psi_{\alpha=0}(t_f)|\psi_\alpha(t_f)\rangle|$. In general, the fidelity increases with increasing g_1, as we shall explain.

We now derive an approximate solution of the time-dependent GPE with the potential in (16). Let us insert the ansatz

$$\tilde{\psi}(q,t) = \exp\left\{\frac{\mathrm{i}}{\hbar}\gamma\,[q - q_\mathrm{c}(t) - \Delta(t), t] + \frac{\mathrm{i}m}{\hbar}\dot{\Delta}(t)q\right\}\psi\,[q - \Delta(t), t]$$

into the GPE, where $\psi(t,q)$ is the solution with the harmonic potential, i.e. $\alpha = 0$, see (7). Then we finally get

$$\frac{\partial\gamma}{\partial t}(y,t) - \mathrm{i}\frac{\hbar}{2m}\frac{\partial^2\gamma}{\partial y^2}(y,t) + \frac{1}{2m}\left[\frac{\partial\gamma}{\partial y}(y,t)\right]^2 - \frac{\mathrm{i}\hbar\frac{\partial\chi}{\partial y}(y)}{m\chi(y)}\frac{\partial\gamma}{\partial y}(y,t) + g_1|\chi(y)|^2\left[1 - \mathrm{e}^{2\mathrm{Im}\gamma(y,t)/\hbar}\right]$$
$$= \tilde{\gamma}(t) + y\left[\frac{6\alpha m\Delta(t)\ddot{q}_c^2(t)}{\omega^2} - 6\alpha m\Delta^2(t)\ddot{q}_c(t) - \frac{2\alpha m\ddot{q}_c^3(t)}{\omega^4} + 2\alpha m\omega^2\Delta^3(t)\right.$$
$$\left. + m\ddot{\Delta}(t) + m\omega^2\Delta(t)\right] + \alpha y^2[\ldots] + \alpha y^3[\ldots] + \alpha y^4[\ldots], \tag{17}$$

where $y := q - q_c(t) - \Delta(t)$ and $\tilde{\gamma}(t)$ is some function that depends only on time. The position expectation value of $\chi(\sigma)$ is $\langle\sigma\rangle = 0$ and so the position expectation value of the unperturbed wavefunction $\psi(q,t)$ is $q_c(t)$. Let the position expectation value of the wavefunction with the perturbed potential be $q_c(t) + \Delta(t)$. We assume that the perturbed wavefunction is non-zero only for $q \approx q_c(t) + \Delta(t)$ and therefore we neglect contributions in the previous equation (17) of orders $\alpha y^2, \alpha y^3, \alpha y^4$. If $\Delta(t)$ is a solution of

$$\ddot{\Delta}(t) = -2\alpha\omega_0^2\Delta^3(t) + 6\alpha\ddot{q}_c(t)\Delta^2(t) - \frac{\omega_0^4 + 6\alpha[\ddot{q}_c(t)]^2}{\omega_0^2}\Delta(t) + \frac{2\alpha[\ddot{q}_c(t)]^3}{\omega_0^4},$$

then the right-hand side of (17) does not depend on y and therefore $\gamma(t,y) = \int_0^y \mathrm{d}t'\,\tilde{\gamma}(t') = \gamma(t)$ is an approximate solution of (17). So we have the approximate wavefunction for the perturbed potential

$$\tilde{\psi}(t,q) = \exp\left[\frac{\mathrm{i}}{\hbar}\gamma(t) + \frac{\mathrm{i}m}{\hbar}\dot{\Delta}(t)q\right]\psi[t, q - \Delta(t)].$$

The approximate perturbed wavefunction should coincide with the unperturbed initial wavefunction at $t = 0$. Therefore we demand the boundary conditions $\Delta(0) = 0$, $\dot{\Delta}(0) = 0$. The effect of the anharmonicity at final time t_f is approximately only a shift $d_{\mathrm{error}} = \Delta(t_f)$ and this shift is independent of g_1. The exact-numerical-final perturbed wavefunction $\psi(t_f,q)$ for different g_1 is shown in figure 2(b) by lines. It coincides very well with the approximated final wavefunction $\tilde{\psi}$ indicated by symbols. In figure 2(b), it can also be seen that the width w of the wavefunction increases with increasing g_1. Because of this, the relative error d_{Error}/w is decreasing for increasing g_1 and this explains why the fidelity is increasing with increasing g_1 in figure 2(a). Using $\tilde{\psi}$, we can approximate the fidelity. This can be further simplified by neglecting $\dot{\Delta}(t_f)$,

$$\tilde{F} = \left|\int \mathrm{d}q\ \chi^*(q)\chi[q - \Delta(t_f)]\right|. \tag{18}$$

This is also shown in figure 2(a) by symbols, and it agrees very well with the exact result.

Finally, we consider the effect of noise in harmonic transport. We assume that the center of the physical trap is randomly perturbed by the shift $\lambda\zeta(t)$ with respect to $q_0(t)$. For the shifted trap center, (10) can be solved using the ansatz $\tilde{q}_c(t) = q_c(t) + \lambda\beta(t)$ so that

$$\beta(t) = \int_0^{\omega_0 t}\mathrm{d}\tau\,\zeta(\tau)\sin(\omega_0 t - \tau), \quad \dot{\beta}(t) = \omega_0\int_0^{\omega_0 t}\mathrm{d}\tau\,\zeta(\tau)\cos(\omega_0 t - \tau),$$

with the solution still given by (7). The fidelity at t_f is

$$\bar{F}_\zeta = \left|\int \mathrm{d}q\ \exp\left[\frac{\mathrm{i}m}{\hbar}\lambda\dot{\beta}(t_f)q\right]\chi^*[q + \lambda\beta(t_f)]\chi(q)\right|. \tag{19}$$

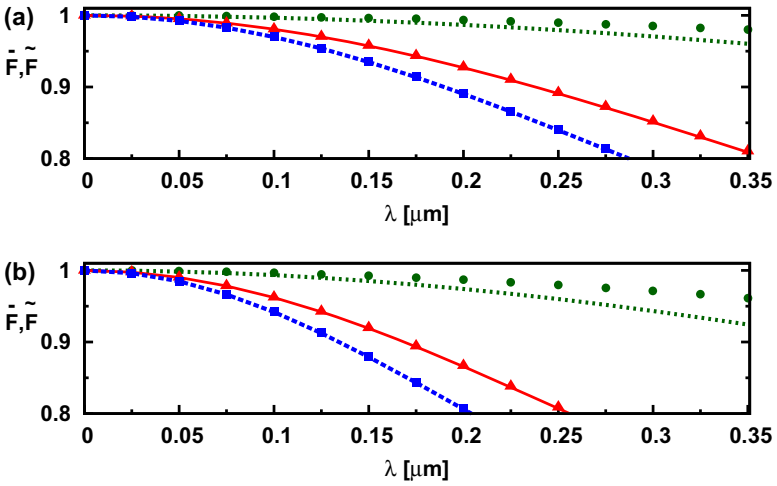

Figure 3. Average fidelity of harmonic transport versus noise intensity λ; (a) $t_f = 10\,\mathrm{ms}$; (b) $t_f = 20\,\mathrm{ms}$. In both cases: the exact result $\bar{F}$ (lines) and approximation $\tilde{F}$ (symbols); $g_1 = 0$ (green dotted lines and circles) and $g_1/\hbar = 0.05\,\mathrm{m\,s^{-1}}$ (red solid lines and crosses), $g_1/\hbar = 0.1\,\mathrm{m\,s^{-1}}$ (blue dashed lines and boxes). $\omega_0 = 2\pi \times 50\,\mathrm{Hz}$.

Quite remarkably, it is independent of d and the chosen $q_c(t)$. We assume now that $\zeta(t)$ is white Gaussian noise, and average the fidelity $\bar{F}_\zeta$ over different realizations of $\zeta(t)$. This exact result $\bar{F} = \langle \bar{F}_\zeta \rangle$ is shown in figure 3 by lines for three values of g_1 and two final times t_f. Note that the result is independent of d. By comparing figures 3(a) and (b), we see that the fidelity increases for shorter times t_f. This can be heuristically understood because the noise has less time to cause perturbations. Moreover, the fidelity increases for smaller couplings g_1, unlike the previous results in figure 2(a). This is because in the noisy perturbation the phase factor $\exp[\frac{im}{\hbar}\lambda\dot{\beta}(t_f)]$, in the above formula (19) for the fidelity, plays an essential role, while the phase factor is negligible in the anharmonic perturbation, see (18). In the noisy perturbation, we may even get a good approximation for the fidelity neglecting the shift $\lambda\beta(t_f)$ completely,

$$\tilde{F}_\zeta = \left| \int \mathrm{d}q \, \exp\left[\frac{im}{\hbar} \lambda \dot{\beta}(t_f) q \right] \chi^*(q) \chi(q) \right| .$$

The average of this approximate fidelity $\tilde{F} = \langle \tilde{F}_\zeta \rangle$ is also shown in figure 3 by symbols and it is a very good approximation for $g_1 > 0$. The approximation $\tilde{F} \approx \bar{F}$ becomes better with increasing g_1 because then the width of the wave function increases and therefore the shift (which is independent of g_1) becomes more and more negligible.

6. Discussion

In this work, we have provided efficient transport protocols for BECs and pointed out the effect of several perturbations. Extensions in several directions may be envisioned: the use of OCT combined with inverse engineering techniques provides a powerful approach and we have given two possible examples minimizing the time for a bounded displacement of the condensate from the trap center or for a bounded accessible space, but there may be many other physical

constraints or conditions that could also be imposed depending on specific settings. A second important open question we leave for future work is to evaluate the effect of the approximate realization of the discontinuities found in some of the optimal (bang–bang) solutions. Moreover, the results of this paper may be extended to other physical scenarios such as non-spherical traps, rotations and launching/stopping condensates up to/from a determined velocity.

Acknowledgments

We thank D Guéry-Odelin for discussions. We acknowledge funding from the Basque Government (grant no. IT472-10) and the Ministerio de Ciencia e Innovación (FIS2009-12773-C02-01). ET acknowledges financial support from the Basque Government (grant no. BFI08.151), and XC from Juan de la Cierva Programme and the National Natural Science Foundation of China (grant no. 60806041).

References

[1] Gustavson T L, Chikkatur A P, Leanhardt A E, Görlitz A, Gupta S, Pritchard D E and Ketterle W 2002 *Phys. Rev. Lett.* **88** 020401
[2] Hänsel W, Hommelhoff P, Hänsch T W and Reichel J 2001 *Nature* **413** 498–501
[3] Schmid S, Thalhammer G, Winkler K, Lang F and Denschlag J H 2006 *New J. Phys.* **8** 159
[4] Xiong D, Wang P, Fu Z and Zhang J 2010 *Opt. Express* **18** 1649
[5] Couvert A, Kawalec T, Reinaudi G and Guéry-Odelin D 2008 *Eur. Phys. Lett.* **83** 13001
[6] Murphy M, Jiang L, Khaneja N and Calarco T 2009 *Phys. Rev.* A **79** 020301
[7] Masuda S and Nakamura K 2010 *Proc. R. Soc.* A **466** 1135
[8] Torrontegui E, Ibáñez S, Ruschhaupt A, Guéry-Odelin D and Muga J G 2011 *Phys. Rev.* A **83** 013415
[9] Chen X, Ruschhaupt A, Schmidt S, del Campo A, Guéry-Odelin D and Muga J G 2010 *Phys. Rev. Lett.* **104** 063002
[10] Schaff J F, Song X L, Vignolo P and Labeyrie G 2010 *Phys. Rev.* A **82** 033430
[11] Muga J G, Chen X, Ruschhaupt A and Guéry-Odelin D 2009 *J. Phys. B: At. Mol. Opt. Phys.* **42** 241001
[12] Schaff J F, Song X L, Capuzzi P, Vignolo P and Labeyrie G 2011 *Eur. Phys. Lett.* **93** 23001
[13] del Campo A 2010 arXiv:1010.2854
[14] Lewis H R and Leach P G 1982 *J. Math. Phys.* **23** 2371
[15] Lohe M A 2009 *J. Phys. A: Math. Theor.* **42** 035307
[16] Song D Y 2005 *Phys. Rev.* A **72** 023614
[17] Song D Y 2006 *Phys. Rev.* A **74** 051602
[18] Lewis H R and Riesenfeld W B 1969 *J. Math. Phys.* **10** 1458
[19] Dhara A K and Lawande S W 1984 *J. Phys. A: Math. Gen.* **17** 2423
[20] Hänsel W, Reichel J, Hommelhoff P and Hänsch T W 2001 *Phys. Rev. Lett.* **86** 608
[21] Günther A, Kemmler M, Kraft S, Vale C J, Zimmermann C and Fortágh J 2005 *Phys. Rev.* A **71** 63619
[22] Dalfovo F, Giorgini S, Pitaevskii L P and Stringari S 1999 *Rev. Mod. Phys.* **71** 463
[23] Couvert A, Jeppesen M, Kawalec T, Reinaudi G, Mathevet R and Guéry-Odelin D 2008 *Europhys. Lett.* **83** 50001
[24] Stefanatos D, Ruths J and Li J S 2010 *Phys. Rev.* A **82** 063422
[25] Pontryagin L S 1962 *The Mathematical Theory of Optimal Processes* (New York: Interscience Publishers)
[26] Salamon P, Hoffmann K H, Rezek Y and Kosloff R 2009 *Phys. Chem. Chem. Phys.* **11** 1027